A theoretical study of Photofield emission in Gallium Arsenide using Kronig-Penney potential model

Leishingthem Nirmala Devi[1] and Ram Kumar Thapa[2]

[1]Condensed Matter Theory Research Group, Physics Department, Mizoram University Aizawl 7896 004, Mizoram India.
[2]Condensed Matter Theory Research Group, Physics Department, Mizoram University Aizawl 7896004, Mizoram India.

nirmalairom18@gmail.com

Abstract. In this report, we have shown the variation of photofield emission current as a function of applied electric field, the photon energy and initial state energy of the electrons with reference to the Fermi level. The photofield emission current is calculated with the help of Kronig- Penney model potential. The origin of peak in photofield emission current in the valence band is explained with the help of result of density of state calculated.

1. Introduction

In this report, we are presenting the calculated results of photofield emission current for gallium arsenide (GaAs) by using Kronig-Penney potential model [1]. PFEC is calculated by using the formula given by Gao and Reifenberger [2]. For the calculation of PFEC, the initial state wavefunction as deduced by Thapa and Kar [1] by using the Kronig-Penney potential model will be used. Dielectric model deduced by Bagchi and Kar [3] is used for obtaining the vector potential. The calculated results of PFEC are plotted as a function photon energy, applied electric field and initial state energy. The maximum peak occurs in the plot of PFEC against initial state energy with respect to Fermi energy is correlated with the plot of density of state (DOS) of GaAs obtained by using density functional theory (DFT) which is implemented in wien2k code [4].

2. Theoretical Formalism

A *p*-polarised radiation of photon energy $\mathrm{h}\omega$ to be incident on the metal surface. This incident radiation, usually a laser beam, causes the transition of electrons from the initial state ψ_i to final state ψ_f. We consider initial states to be electron states lying below the Fermi level, and final states are states in the vacuum (detector). Therefore, the photofield emission current density measured can be written Gao and Reifenberger as [2].

$$\frac{dj}{dE} = -\frac{e^3}{2\mathrm{h}^4\omega^3}\frac{n}{\Omega}(\hat{\varepsilon}.\hat{z})^2 f\left(E-\mathrm{h}\omega\right)\int_{-V_o+\mathrm{h}\omega}^{E} dW \frac{D(W)\left|M_{fi}\right|^2}{\left[W\left(W-\mathrm{h}\omega\right)\right]^{\frac{1}{2}}} \tag{1}$$

Where $\frac{n}{\Omega}(\hat{\varepsilon}.\hat{z})^2 = \left|\frac{A_\omega(z)}{A_0}\right|^2 = \left|\tilde{A}_\omega(z)\right|^2$, and $A_\omega^z(z)$ is the *z*-component of vector potential along *z*-axis, A_0 is the amplitude of vector potential associated with the incident radiation, $f(E-\hbar\omega)$ is the Fermi-Dirac distribution function, *D(W)* is the quantum mechanical transmission probability and the energy of the photo-excited electrons is $E_{KIN} = W + \frac{\hbar^2 k_\parallel^2}{2m}$, where *W* is the normal component of kinetic energy E_{KIN}. These electrons will travel across the surface potential barrier which is deformed by the applied electrostatic field and the image potential barrier. At first we will discuss the various parameters involve in Eq. (1).

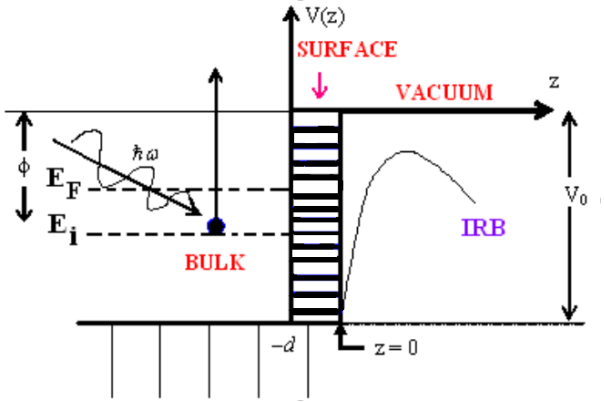

Figure 1. Model potential used for photofield emission calculation. Here E_i is the Fermi level E_i is the initial state energy of the electron, IRB is the image rounded barrier potential, V_0 is the potential barrier.

Matrix element M_{fi} in Eq. (1) due to transition of electrons from the initial state $|\psi_i>$ to the final state $|\psi_f>$ is

$$M_{fi} = \langle f | \boldsymbol{A}.\boldsymbol{p} + \boldsymbol{p}.\boldsymbol{A} | i \rangle \tag{2}$$

Now for Hamiltonian, $\boldsymbol{H} = \frac{\boldsymbol{p}^2}{2m} + V$ where momentum operator $p = -i\hbar\Delta$, the commutator $\boldsymbol{A.p}$ with the Hamiltonian $\boldsymbol{H}$ is given by,

$$[\boldsymbol{A.p}, \boldsymbol{H}] = -i\hbar\,\boldsymbol{A}.\nabla V + \frac{\hbar^2}{2m}\nabla^2(\boldsymbol{A}.\boldsymbol{p}) + \frac{i\hbar}{m}\nabla(\boldsymbol{A}.\boldsymbol{p}).\boldsymbol{p} \tag{3}$$

From Eq. (2) and Eq. (3), we have

$$M_{fi} = \frac{2i}{\omega}\langle f | \boldsymbol{A}.\nabla V | i \rangle + \frac{\hbar}{m\omega}\langle f | \nabla^2 \boldsymbol{A}.\boldsymbol{p} | i \rangle - \frac{2i}{\omega}\langle f | \nabla.(\boldsymbol{A}.\boldsymbol{p}).\boldsymbol{p} | i \rangle - i\hbar\langle f | \nabla.\boldsymbol{A} | i \rangle \tag{4}$$

In Eq. (4), $V = V_B + V_S$, where V_B and V_S are the bulk and surface potentials. In photofield emission, the dominant contribution to the current comes from the surface photo effect. In Eq. (4), the effective potential is given by

$$V(z) = \begin{cases} -V_0 - eFz - \frac{e^2}{4z}, & for\ z > 0 \\ 0 \quad , & for\ z < 0 \end{cases} \tag{5}$$

where $V(z)$ is called image rounded potential barrier.

To evaluate the Initial state wave functions $\psi_i(z)$, one solves the one-dimensional Schrodinger equation

$$\frac{d^2\psi(z)}{dz^2} + k_i^2\,\psi(z) = -2\,V(z)\,\psi(z) \tag{6}$$

where $k_i^2 = 2E_i$ and $V(z)$ is the δ-function potential of the Kronig-Penney (K-P) model.

Let $\phi(z)$ denote the Bloch wave function deep inside the metal and $\phi^*(z)$ the time version of $\phi(z)$. The eigenfunction in the semi-infinite solid $(z<0)$ was chosen to have the form

$$\psi_i(z) = \phi(z) - P\phi^*(z) \tag{7}$$

Where *P* is the reflection coefficient obtained by matching the wave function and its derivative at z = 0. The initial state wavefunction for z < 0 may be written as

$$\psi_i(z) = \left(1 - iP\,e^{-i\delta}\sin\delta\right)e^{i\,k_i\,z} - \left(P - ie^{-i\,\delta}\sin\delta\right)e^{-i\,k\,z} \tag{8}$$

Where $\cot\delta = \frac{k_i}{g}$, g being the strength of the potential. The Initial state wave functions outside the metal (z > 0) is

$$\psi_i(z) = Te^{-\chi\,z} \tag{9}$$

Where T being the transmission coefficient across the boundary plane and

$$\chi^2 = 2\,(V_0 - E_i) \tag{10}$$

Where V_0 is the surface step potential, the matching boundary conditions at z = 0 is given as

$$P = \frac{(\chi - ik_i) - (k_i - i\chi)\,e^{i\delta}\sin\delta}{(\chi - ik_i) + (k_i - i\chi)\,e^{-i\delta}\sin\delta} \tag{11}$$

$$T = \frac{2k_i\sin 2\delta}{(\chi - ik_i) + (k_i - i\chi)\,e^{-i\delta}\sin\delta} \tag{12}$$

and the final state wave functions $\psi_i(z)$ is given by

$$\psi_f(z) = \begin{cases} \left(\frac{1}{2\pi\,q}\right)^{\frac{1}{2}} \frac{2q}{q+k_f}\,e^{i\,k_f z}, & z<0\ (bulk\ \&\ surface) \\ \left(\frac{1}{2\pi\,q}\right)^{\frac{1}{2}} \left[e^{i\,q\,z} + \left(\frac{q-k_f}{q+k_f}\right)\right]e^{-iqz}, & z>0\ (vacuum) \end{cases} \tag{13}$$

where, $k_f{}^2 = 2E_i$, $q^2 = 2(E_f - V_0)$ *and* $E_f = E_i + \mathrm{h}\omega$.

The matrix element M_{fi} in Eq. (4) when expanded in one-dimension along *z*-axis is given by,

$$M_{fi} = \int_{-d}^{0}\psi_f^* A_z\frac{dV}{dz}\psi_i dz + \int_{-d}^{0}\psi_f^*\frac{d^2A_z}{dz}\left(-\mathrm{i}\mathrm{h}\frac{d}{dz}\right)\psi_i dz + \int_{-d}^{0}\psi_f^*\frac{dA_z}{dz}\left(-\mathrm{h}^2\frac{d^2}{dz^2}\right)\psi_i dz + \int_{-d}^{0}\psi_f^*\frac{dA_z}{dz}\psi_i dz \tag{14}$$

Here A_z is the z-component of vector potential along z-axis. A_z will be the one used by Thapa and Das [5] for calculating PFEC in the case of W.

The transmission tunneling probability *D(W)* used in Eq. (1) has been calculated Thapa *et al*.[5] by solving the Airy's differential equation and matching the wave functions inside and outside the surface at *z* = 0.0. The standard form of Airy's differential equation is

$$D(W) = \frac{W^{\frac{1}{4}}\sqrt{\pi}}{(heF)^{\frac{1}{6}}}\left(\frac{2ik_i}{ik_i+\chi}\right)(2m)^{\frac{1}{12}}\exp\left[-i\left(\frac{2}{3}\frac{W^{\frac{3}{2}}\sqrt{2m}}{heF}+\frac{\pi}{4}\right)\right] \quad (15)$$

The wavefunction given by Eq. (8) and Eq. (13) are then used in Eq. (1) to calculate PFEC by writing FORTRAN program.

3. Results and Discussions

We report here the calculated results of photofield emission current (PFEC) of gallium arsenide (GaAs) obtained by using the Kronig-Penney potential model. PFEC is calculated as a function of initial state energy (E_i), photon energy ($\hbar\omega$) and the applied high static electric field (F) at surface and bulk region. The input parameters used for calculations of PFEC are: surface width (d) = 5.7363 A^0, initial state energy (E_i) = 4.4988 eV, potential barrier height (V_0) = 10.2562 eV, work function (ϕ) = 4.69 eV, Fermi energy (E_F) = 5.5662 eV, scattering factor (α) = 0.35 and phase shift (δ) = -0.6416.

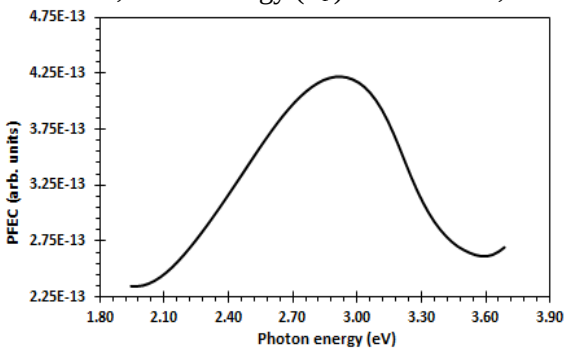

Figure 2. Plot of variation of PFEC against the photon energy. The angle of incident photon radiation is $\theta_i = 45^0$ and surface width (d) = 5.7363A^0.

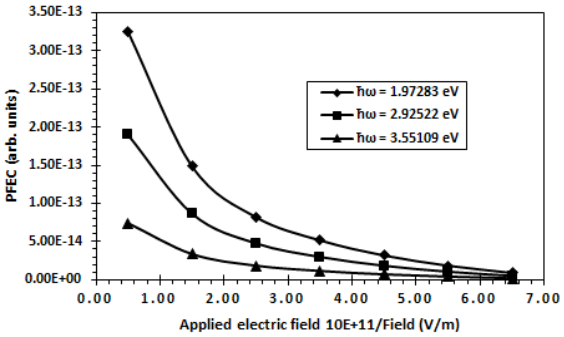

Figure 3. Plot of variation of PFEC against the applied electric field for three different values of photon energies and the angle of incident photon radiation is $\theta_i = 45^0$.

In Fig. 2, we have plotted the calculated results of calculated PFEC for GaAs as a function of photon energy $\hbar\omega$. In this case, we have taken applied electric field (F) is equal to 1.6 x 10^{11} V/m and calculated PFEC for photon energy in a range of $\hbar\omega$ = 1.80 – 3.90 eV. Here we have chosen the initial state energy E_i = 1 eV below Fermi level (E_F = 0.0). From the plot we have seen that the PFEC is increased as increase of photon energy. It shows a maximum at photon energy 2.925 eV. With the further increase in photon energy PFEC decreases and it becomes minimum at around $\hbar\omega$ = 3.60 eV.

In Fig. 3, we have plotted the calculated results of PFEC as a function of the applied electric field (F) for three difference values of photon energies $\hbar\omega$ = 1.97283 eV, 2.92522 eV and 3.55109 eV respectively. We have chosen the initial state energy E_i = 1 eV below Fermi level (E_F = 0.0). From the plot, we have seen that the value of applied electric field when increase the PFEC decreased from a high value towards minimum in an exponential manner for all the three different values of photon energies. The exponential decrease in PFEC is due to reason that an exponential term is present in calculation of transition probability $D(W)$ given by Eq. (15). From this plot we have also seen that, the value of PFEC maximum for low photon energy $\hbar\omega$ = 1.97283 eV and the value of PFEC minimum for large photon energy $\hbar\omega$ = 3.55109 eV. This is due to the reason that PFEC given in Eq. (1) is inversely proportional to cube of frequency of incident photon radiation. However, the variation of PFEC in all the cases of three different values of photon energies are similar in nature.

In Fig. 4, we have plotted the results of the calculated PFEC as a function of initial state energy (E_i) for three difference values of photon energies $\hbar\omega$ = 1.97283 eV, 2.92522 eV and 3.55109 eV respectively. Here the value of applied electric field (F) is equal to 1.6 x 10^{11} V/m. and initial state energy E_i is chosen below the Fermi level (E_F = 0.0). From the plot, we have seen that PFEC for

photon energy $\hbar\omega$ = 1.97283 eV shows a peak at initial state energy E_i = 2.45 eV below the Fermi level. With the further decrease in initial state energy PFEC also decreases and minimum at around E_i = 2.65 eV below the Fermi level. We have also plotted in the same Fig. 4 the calculated results of the

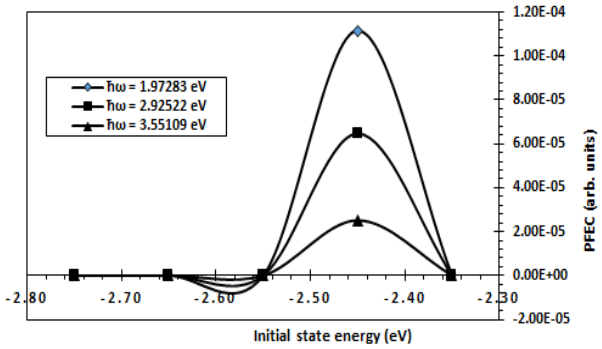

Figure 4. Plot of variation of PFEC against the initial state energy for three values of photon energies. The Fermi energy E_F = 0.0 is taken as reference level and the angle of incident photon radiation is $\theta_i = 45^0$.

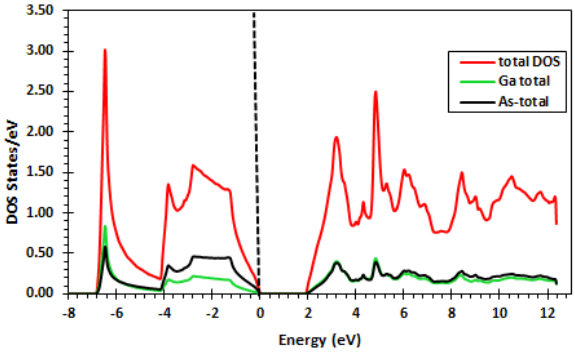

Figure 5. Plot of Total DOS for GaAs, Ga and As. Fermi level is at 0.

PFEC for photon energies $\hbar\omega$ = 2.92522 eV and 3.55109 eV respectively. From this plot, we have also seen that maxima in PFEC occur at same initial state energy that is, E_i = 2.45 eV for both photon energies 2.92522 eV and 3.55109 eV below Fermi level respectively. Here the peak in PFEC is higher for low photon energy $\hbar\omega$ = 1.97283 eV than for photon energies 2.92522 eV and 3.55109 eV. Therefore, the large value of PFEC for low photon energy value $\hbar\omega$ = 1.97283 eV whereas low value of PFEC for high photon energy $\hbar\omega$ = 3.55109 eV. This is the reason that PFEC is inversely proportional to cube of frequency of incident photon radiation as given in Eq. (1). In all the three cases we find that with the further lowering of initial state energy beyond the peaks occurrence, the values of PFEC decreases exponentially.

The total DOS plot for GaAs, Ga and As is shown in fig. 5. In this plot Fermi level is taken at 0. The maximum peak occurs at 6.45 below the Fermy level is neglected due to occurrence of peak in core region. The second maxima in total DOS of GaAs occurs at 2.77 eV in valence region below the Fermi level. In valence region most of the contribution are coming from *s* and *p*-states electrons of Ga and *p*-state electrons of As atoms. However to compare the contribution of Ga and As atoms, *p*-state electrons of As atom is more contributing than *p*-state electrons of Ga atom. This is evident from partial DOS plots of GaAs [6].

The origin of peaks occurred at 2.45 eV below the Fermi level as shown in Fig. 4 can be correlated with the occurrence of the maxima at 2.77 eV in the total DOS plot for GaAs, Ga and As which is shown in Fig. 5. This means that the origin of peaks at 2.45 eV below the Fermi level as shown in Fig. 4 is due to contribution by *s* and *p*-states of Ga and *p*-state of As. This is evident from the partial DOS plots of Ga and As atoms where the maximum in DOS was contributed by Ga-*s* and *p* and As-*p* states electrons [6].

4. Conclusions

In calculating PFEC we have used the Kronig-Penney potential model which have been used by Thapa and Kar [1]. It is found that the behaviour of PFEC as a function of applied field and initial state energy shows similar trends also in the case of GaAs. The occurrence of peak in PFEC at initial state E_i = 2.45 eV below the Fermi energy can be addressed due to band structure effects. This is evident from the plots of density of state (DOS) in GaAs which is shown in Fig. 5. However the discrepancy in the location of peaks as shown in Fig. 3 and Fig. 4 can be attributed to the choice of the

wavefunctions to evaluate the matrix element. However, few drawbacks are still existing which must be attended for better accuracy. For example, we have used the real and imaginary dielectric constants which had been calculated by using the density functional theory. This was included to the model as proposed by Bagchi and Kar [3]. We are trying to correlate appropriately the dielectric model in the context of density function theory to calculate vector potentials for transition probability.

Acknowledgments
I am grateful to Mizoram University UGC fellowship, RKT acknowledges a grant from SERB (DST, India) via grant No. EMR/2015/001407, Dt.11th March 2016.

References

[1] Thapa R K and Kar N 1988, "Photoemission calculation from band States using Kronig-Penny model and spatially varying photon field," *Indian J. Pure. Appl. Phys.* **26** 620-623
[2] Gao Y and Reifenberger R 1987, "Photofield emission from transition-metal surface states," *Phys. Rev.* B **35** 4284-4290
[3] Bagchi A and Kar N 1978, "Reflection effects in angle-resolved Photo emission from surface states on metal," *Phys. Rev.* B **18** 5240-5247
[4] Blaha P, Schwarz K, Madsen G K H, Kvasnicka D and Luitz J 2015, "An augmented plane wave plus local orbitals program for calculating crystal properties, in: WIEN2K", *Vienna Universitat of Technology*, Vienna
[5] Thapa R K and Gunakar Das 2005, "A simple theory of photofield emission from the surface of a metal," *Intl. Jour. Mod. Phys.* B **19** 3141-3149
[6] Nirmala devi L, and Thapa R K, "study of electronic and optical properties of Gallium arsenide (GaAs) by using Full-Potential Linearized Augmented Plane Wave Method (FP-LAPW), "unpublished"
[7] Nirmala devi L and Thapa R K 2016, "Study of Photofield emission in GaAs using Kronig-Penney model," *Journal of Materials Science and Engineering*, A **6 (3-4)** 110-112
[8] Thapa Ram Kumar, Nirmala Devi L, Benjamin Vanlalruata, Rebecca Lalngaihawmi, Amit Shankar, Sandeep Chettri, Dibya Prakash Rai and Ghimire M P 2015 *Proc. 2015 International Conference on Electrical and Electronics: Techniques and Applications (EETA 2015)* (Phuket, Thailand) pp 53-57